STATISTICS, OPTIMIZATION AND INFORMATION COMPUTING
Stat., Optim. Inf. Comput., Vol. **x**, Month 202x, pp 0–25.
Published online in International Academic Press (www.IAPress.org)

Modeling Lifetime and Reliability Data Using the Inverse Power Induced Ailamujia Distribution

Mohammed Elgarhy [1,2], Fatimah Alrefeadi [3,*], Ahmed Mohamed El Gazar [4], Dina A. Ramadan [5]

[1] *Faculty of Computers and Information Systems, Egyptian Chinese University, Nasr City, Egypt (Mohammed.Elgarhy@ecu.edu.eg)*
[2] *Department of Computer Engineering, Biruni University, 34010, Istanbul, Turkey*
[3] *Department of Mathematics, Al-Qunfudah University College, Umm Al-Qura University, Makkah, Saudi Arabia (farefaidi@uqu.edu.sa)*
[4] *Department of Basic Sciences, Higher Institute for Commercial Sciences, Almahlla Alkubra, Egypt (a.elgazar99@gmail.com)*
[5] *Department of Mathematics, Faculty of Science, Mansoura University, Mansoura 35516, Egypt (Dinaramadan21@mans.edu.eg)*

Abstract This study introduces a new and flexible lifetime model, named the inverse power induced Ailamujia (IPIA) distribution, developed by integrating the inverse power transformation into the classical induced Ailamujia framework. The suggested model is aimed at improving the flexibility of lifetime data analysis and at providing a more accurate depiction of complicated real-world phenomena characterized by skewness and changeable hazard rate patterns. The basic statistical features of IPIA distribution including probability density function (PDF), cumulative distribution function (CDF), moments, quantile function and entropy measures are computed. In this study, we perform a comprehensive Monte Carlo simulation to evaluate and compare the effectiveness of multiple techniques of parameter estimation, namely maximum likelihood (MLE), Bayesian (BE) and maximum product of spacings (MPS) methods. To illustrate the practical usage of the suggested IPIA model we fit it to two real world datasets from the economic and the maintenance engineering domains. The results highlight the superiority of the IPIA model over several existing distributions in terms of fit quality and flexibility.

Keywords Induced Ailamujia distribution, Inverse power transformation, Moments, Quantile function, Bayesian estimation method, Real datasets

AMS 2010 subject classifications 60E05, 62E10, 62F10, 62F15

DOI: 10.19139/soic-2310-5070-4906

1. Introduction

In essence, statistical inference is the use of probability distributions to make inferences about real-world data. These mathematical models provide a formal method of analyzing random variables and measurement of the quantity of variation in the sample data. The investigator can then systematically estimate unknown parameters using a credible model, test substantial hypotheses about the data producing process, and compare competing distributions to see which best reflects the real-world situation under consideration. These are processes of real application in healthcare, engineering, biology and economics, not only of theoretical interest.

We usually use the inverse power transformation in constructing flexible probability models, particularly when data are highly skewed or possess heavy tails that are difficult to model with standard formulations. A similar inverse framework is particularly useful when used with non-monotone hazard rate functions, including a bathtub curve, a unimodal trajectory or the classic upside-down bathtub pattern, which are common in reliability engineering and biomedical settings where the concept of a monotonic hazard is often biologically or physically

*Correspondence to: Fatimah Alrefeadi (Email: farefaidi@uqu.edu.sa). Department of Mathematics, Al-Qunfudah University College, Umm Al-Qura University, Makkah, Saudi Arabia.

ISSN 2310-5070 (online) ISSN 2311-004X (print)
Copyright © 202x International Academic Press

unfounded. Furthermore, the technique naturally handles heavy tails. This is a desirable feature for the analysis of long-tailed survival data, where the risk level does not plateau. Several inverse distributions have been proposed, and they can be grouped by the feature they were designed to capture. For heavy-tailed survival data, the inverse power Lindley [3], inverse power Lomax [10], inverse power Zeghdoudi [13], and inverse power Cauchy [12] extend classical heavy-tailed families through an inverse power transformation; they provide flexible tails but either lack closed-form moments or do not nest a baseline induced distribution. For bounded or semi-bounded support, the inverse Kumaraswamy [4], inverse Topp-Leone [7], and inverse XLindley [15] offer alternative hazard shapes but are not directly comparable to models on $(0, \infty)$. For non-monotone hazards, the inverse exponentiated Weibull [9] and inverse exponentiated Lomax [5] provide unimodal shapes, at the cost of additional parameters. None of these families simultaneously (i) nests the induced Ailamujia baseline, (ii) retains closed-form expressions for moments, quantile function, and entropy, and (iii) produces increasing, decreasing, and unimodal hazards with only two parameters.

The inverse method is not some arcane, theoretical mathematical device that is of no utility. This is a practical method of dealing with data when the hazard rate function is not willing to be monotonic, whether it is the classic bathtub curve, a rise and fall that is unimodal or the less common upside-down bathtub (UBT) pattern encountered in practice. In fields such as oncology or mortality studies the monotonic hazard assumption is often little more than a convenient oversimplification.

The baseline Induced Ailamujia (IAL) distribution can be interpreted structurally as an equal-weight mixture of an exponential distribution and an Erlang distribution with shape parameter 2. While the IAL framework offers basic non-monotonic hazard flexibility, its single scale parameter restricts tail weight and skewness modeling.

The proposed Inverse Power Induced Ailamujia (IPIA) model applies the transformation $w = y^{-1/\beta}$ to the baseline $Y \sim \mathrm{IAL}(\alpha)$. This introduces a distinct structural shape parameter $\beta > 0$ that fundamentally alters the tail behavior and hazard rate shapes compared to previously published inverse-power Ailamujia variants. For more details see [1, 2, 6, 8, 11, 14, 40–42].

The Ailamujia (AL) distribution [16] was originally proposed as a viable distribution for positively skewed survival and biological data, but has since become a family of extended models, such as size-biased, area-biased, weighted, inverse and truncated inverse power models [17–24], to accommodate certain features in data that the baseline model may not capture. From a mathematical standpoint, the AL model may be viewed as a constrained special case of the Erlang distribution, where the shape parameter is fixed at a value of two and the rate parameter is denoted by α. Reparameterization to $\alpha = 1/\gamma$ (where $\gamma > 0$) results in the well-known length-biased exponential distribution [25]. The AL model is a strong and practical alternative to the traditional single-parameter baselines such as the Lindley and exponential distributions [26], particularly when the data demand something more flexible than the simplest options. When presenting our recommended approach, we need to first lay out basic equations for the inverse Ailamujia (IAL) distribution [27], a univariate model defined under the parametric constraint α, allowing us a feasible and mathematically feasible way to represent the patterns we usually identify in non-monotonic survival data, to that end, the probability density function (PDF) and the cumulative distribution function (CDF) for this distribution take the following forms:

$$f(y;\alpha) = \alpha\,(1 + 2\alpha y)\,e^{-2\alpha y}, \tag{1}$$

and

$$F(y;\alpha) = 1 - (1 + \alpha y)\,e^{-2\alpha y}, \tag{2}$$

where α is the scale parameter.

The IAL distribution has a highly desirable feature: all its fundamental values like PDF, CDF, survival rate, hazard function, quantiles and moments are available in closed form. Therefore, it can be easily adapted to increase, decrease or bathtub shaped risk behaviors as per the data needs. The IAL distribution is a one-parameter model for positively skewed survival data, but its single parameter limits the range of hazard shapes it can produce. Adding a shape parameter through the inverse power transformation addresses this limitation while preserving the analytical tractability of the baseline. The resulting IPIA model is therefore a two-parameter family that is both flexible and analytically tractable, and it fills the gap identified above.

The rest of this paper is structured in seven sections addressing a different component of the overall framework. In Section 2 we begin by discussing the structural development of the suggested distribution and in Section 3 we go on to discuss its basic mathematical features in some depth. Section 4 looks at the practical problem of parameter estimation, discussing a number of potential methodologies. Section 5 evaluates these estimators in an extended Monte Carlo simulation exercise. In Section 6 we evaluate the model in reality by applying it to two real-world datasets from distinct application fields, and we conclude in Section 7 where we summarize the key results we have found and indicate some intriguing directions for further research.

2. Inverse Power Induced Ailamujia Distribution

In this part we derive the mathematical expression for the IPIA distribution, which generalizes the baseline IAL model by including an additional shape parameter. In addition to its analytical formulation, we include graphical demonstrations of the PDF and the CDF. The support of $w = y^{-1/\beta}$, as $(0, \infty)$, is then obtained by solving for y at $y = 0$ and $y = \infty$, respectively. Assuming that $y = w^{-\beta}$ represents the observed value of Y, then $y = w^{-\beta}$ and $\frac{dy}{dw} = -\beta\, w^{-\beta-1}$. The IPIA model is built by applying the transformation $W = Y^{-1/\beta}$, where Y represents a random variable governed by the IAL distribution with the CDF specified in Eq. (2). The resulting mathematical expressions for the PDF and CDF are formulated as below:

$$f(w;\alpha,\beta) = \alpha\beta\, w^{-\beta-1}\left(1+2\alpha w^{-\beta}\right) e^{-2\alpha w^{-\beta}}, \tag{3}$$

and

$$F(w;\alpha,\beta) = \left(1+\alpha w^{-\beta}\right) e^{-2\alpha w^{-\beta}}, \tag{4}$$

where α is the scale parameter and β is the shape parameter.

Figure 1 visually captures the behavioral flexibility of the IPIA model across different lifetime scenarios through its PDF and CDF plots. The PDF is increasing, decreasing, right skewed, and unimodal, while the plot of CDF takes increased trend.

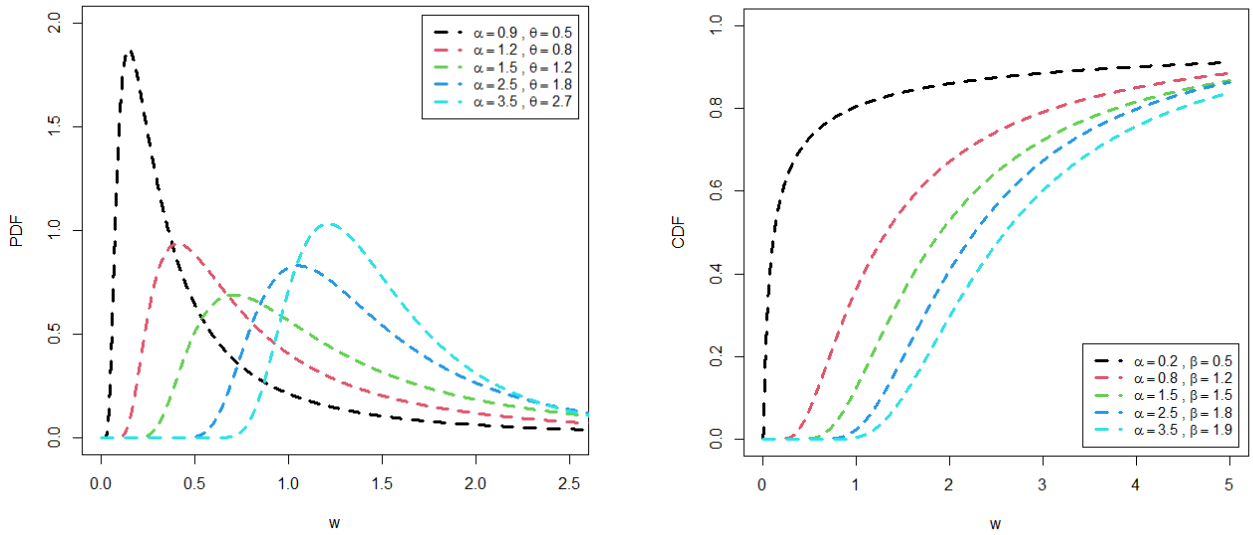


Figure 1. Some plots of the PDF and CDF of the IPIA model at different values of parameters.

The survival function (SF) measures the probability of a system persisting beyond a specified time limit, whereas the hazard rate function (HRF) exhibits the immediate danger of failure at that precise moment. The mathematical equations that dictate both the SF and HRF for the suggested IPIA distribution are defined as follows:

$$S(w;\alpha,\beta) = 1 - \left(1+\alpha w^{-\beta}\right) e^{-2\alpha w^{-\beta}}, \tag{5}$$

and

$$h(w;\alpha,\beta)=\frac{\alpha\beta\, w^{-\beta-1}\left(1+2\alpha w^{-\beta}\right)e^{-2\alpha w^{-\beta}}}{1-\left(1+\alpha w^{-\beta}\right)e^{-2\alpha w^{-\beta}}}. \tag{6}$$

Figure 2 illustrates the survival and hazard functions of the IPIA under various failure conditions. Survival diminishes from 1 to 0 over time, faster with low values of the parameters α, β and more gradually with high ones, while the hazard rate increases as these parameters grow, reflecting the system's inherent aging and decline.

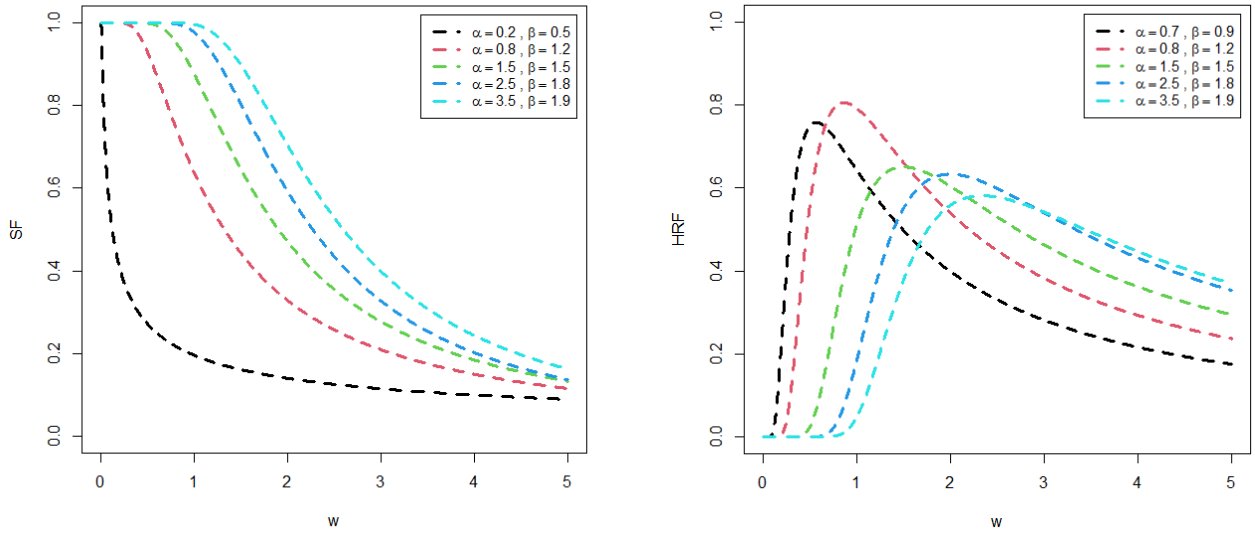


Figure 2. Survival and hazard rate function plots of the IPIA model for different values of the parameters α and β.

Asymptotic behavior discussion. As $w\to 0$, $f(w)\to 0$ and $h(w)\to 0$, whereas as $w\to\infty$, $f(w)\to 0$ with severe right skewness. The asymptotic behavior of the hazard rate is dominated by the power-law tail, yielding $h(w)\sim\beta/w$ as $w\to\infty$, which confirms an upside-down trend or declining hazard pattern rather than a standard monotonic.

3. Mathematical and Statistical Properties of the IPIA Distribution

In this study, the basic statistical properties of the IPIA distribution are developed, and the reliability characteristics, moments, moment generating function and measures of information entropy are explicitly derived.

3.1. Quantile Function

The quantile function (QF) is a basic analytical tool for the evaluation of the structural properties of a probability distribution and the determination of its specific percentiles. For the case of a random variable W that follows IPIA distribution, the QF is obtained by inverting the CDF given by Eq. (4) and equating it to u, where u is uniformly distributed in the interval $(0,1)$. The relationship can be summarized as follows:

$$Q(u)=\left[-\frac{1}{\alpha}-\frac{1}{2\alpha}\,W_{-1}\left(-2u\,e^{-2}\right)\right]^{-1/\beta},\qquad u\in(0,1), \tag{7}$$

where $W_{-1}(\cdot)$ represents the negative branch of the Lambert W function.

The quantile function of the IPIA distribution can be obtained simply from Eq. (7). Substituting $u=0.25$, 0.5, and 0.75 in Eq. (7), we get the first quantile (Q_1), the median (Q_2), and the third quantile (Q_3) correspondingly. Additionally, Bowley's skewness (ρ_1) and Moors' kurtosis (ρ_2) can be computed using these quantiles. A

significant advantage of these measures is their simplicity, because the calculation of them does not need the existence of traditional moments.

Table 1 shows the performance of the quantile-based statistics involving Q_1, Q_2, Q_3, ρ_1, and ρ_2 for different values of parameters α and β of the IPIA model. The results indicate that the placements of the quantiles and the related skewness and kurtosis values differ greatly depending on the value of α or β. As α increases, the skewness of the model generally decreases, leading the distribution towards a more symmetric profile, and as β increases, the kurtosis is boosted, indicating a larger weight of the tail.

Interpretation of quantile measures. As shown in Table 1, quantile-based robust measures (Bowley's skewness ρ_1 and Moors' kurtosis ρ_2) depend solely on the shape parameter β and are invariant to changes in the scale parameter α. Furthermore, increasing β leads to a systematic reduction in both skewness and kurtosis.

3.2. Moments

Moments are basic definitions in statistical modeling to comprehend basic features of a probability distribution, such as its central location, dispersion, and asymmetry. When we measure these mathematical assumptions, we acquire insight into the structural geometry of the distribution and its spread. These insights are of crucial relevance when we evaluate risk in finance, quality control measurements, and environmental trends. Let W be a random variable with the associated PDF of the IPIA distribution specified in Eq. (3). The general equation for the μ'_r is given by:

$$\mu'_r = \int_0^\infty w^r \, f(w;\alpha,\beta)\, dw. \tag{8}$$

From Eq. (3) in Eq. (8), we have

$$\mu'_r = \int_0^\infty w^r \, \alpha\beta \, w^{-\beta-1} \left(1 + 2\alpha w^{-\beta}\right) e^{-2\alpha w^{-\beta}} \, dw.$$

By substituting $z = 2\alpha w^{-\beta}$, i.e. $w = (2\alpha)^{1/\beta} z^{-1/\beta}$ and $dw = -\frac{1}{\beta}(2\alpha)^{1/\beta} z^{-\frac{1}{\beta}-1}\, dz$, then

$$\begin{aligned}
\mu'_r &= \frac{1}{2}(2\alpha)^{r/\beta} \int_0^\infty \left[z^{-r/\beta} e^{-z} + z^{-r/\beta+1} e^{-z} \right] dz \\
&= \frac{1}{2}(2\alpha)^{r/\beta} \left[\Gamma\left(1 - \frac{r}{\beta}\right) + \Gamma\left(2 - \frac{r}{\beta}\right) \right], \qquad r < \beta,
\end{aligned} \tag{9}$$

by using the gamma function, $\Gamma(z) = \int_0^\infty t^{z-1} e^{-t}\, dt$.

Furthermore, the analytical expressions for the skewness (ρ_3), kurtosis (ρ_4), and coefficient of variation (ρ_5) corresponding to the IPIA model are derived as follows:

$$\rho_3 = \frac{\mu'_3 - 3\mu'_1\mu'_2 + 2(\mu'_1)^3}{(\sigma^2)^{3/2}}, \qquad \rho_5 = \frac{(\sigma^2)^{1/2}}{\mu'_1},$$

and

$$\rho_4 = \frac{\mu'_4 - 4\mu'_1\mu'_3 + 6\mu'_2(\mu'_1)^2 - 3(\mu'_1)^4}{(\sigma^2)^2}.$$

Table 2 presents the computed numerical results for the main statistical moments and parameters of the IPIA distribution. The findings are the variance (σ^2), ρ_3, ρ_4, and the initial four moments μ'_1, μ'_2, μ'_3, and μ'_4. As magnitudes of the parameters α and β increase, an inverse link may be observed that systematically reduces the computed value of moments and discrete geometric changes in the distribution. This pattern highlights the strong dependence of the IPIA framework on its parameter space, showing how these coefficients control the full statistical behavior of the model. Also, Figure 3 displays three-dimensional surface plots of the foundational statistical metrics of the IPIA model, specifically tracking the mean, variance, skewness (ρ_3), kurtosis (ρ_4), coefficient of variation (ρ_5), and index of dispersion (ρ_6).

Table 1. Variation of quantile measures of the IPIA model with respect to α and β

α	β	Q_1	Q_2	Q_3	ρ_1	ρ_2
0.2	4.5	0.6914	0.7914	0.9442	0.2086	1.3964
	5.0	0.7174	0.8101	0.9496	0.2011	1.3847
	5.5	0.7394	0.8258	0.9541	0.1950	1.3756
	6.0	0.7582	0.8391	0.9578	0.1898	1.3684
0.4	4.5	0.8065	0.9232	1.1014	0.2084	1.3962
	5.0	0.8240	0.9306	1.0908	0.2013	1.3849
	5.5	0.8387	0.9367	1.0822	0.1951	1.3758
	6.0	0.8511	0.9418	1.0751	0.1898	1.3682
0.6	4.5	0.8826	1.0102	1.2053	0.2086	1.3963
	5.0	0.8936	1.0092	1.1830	0.2011	1.3847
	5.5	0.9028	1.0084	1.1650	0.1950	1.3757
	6.0	0.9106	1.0077	1.1503	0.1900	1.3683
0.8	4.5	0.9408	1.0769	1.2848	0.2085	1.3962
	5.0	0.9466	1.0690	1.2530	0.2011	1.3848
	5.5	0.9513	1.0625	1.2276	0.1949	1.3759
	6.0	0.9553	1.0572	1.2068	0.1897	1.3681
0.9	4.5	0.9658	1.1055	1.3189	0.2086	1.3963
	5.0	0.9691	1.0945	1.2829	0.2011	1.3849
	5.5	0.9719	1.0855	1.2542	0.1949	1.3755
	6.0	0.9742	1.0781	1.2307	0.1898	1.3683
1.2	4.5	1.0295	1.1785	1.4059	0.2085	1.3965
	5.0	1.0265	1.1593	1.3589	0.2010	1.3849
	5.5	1.0241	1.1438	1.3215	0.1949	1.3755
	6.0	1.0221	1.1311	1.2912	0.1900	1.3682
1.5	4.5	1.0819	1.2384	1.4774	0.2086	1.3963
	5.0	1.0734	1.2122	1.4209	0.2010	1.3848
	5.5	1.0665	1.1912	1.3763	0.1949	1.3755
	6.0	1.0608	1.1740	1.3401	0.1895	1.3684
1.8	4.5	1.1266	1.2896	1.5385	0.2085	1.3962
	5.0	1.1133	1.2572	1.4736	0.2011	1.3849
	5.5	1.1024	1.2313	1.4226	0.1949	1.3756
	6.0	1.0935	1.2102	1.3815	0.1898	1.3670

Existence constraints. The existence of the r-th raw moment strictly requires $\beta > r$. Therefore, the theoretical mean, variance, skewness, and kurtosis exist only when $\beta > 1$, $\beta > 2$, $\beta > 3$, and $\beta > 4$, respectively. Table 2 and Figure 3 have been updated to reflect only parameter sets satisfying $\beta > 4$.

Table 2. Computed values of the moments and associated statistical measures for the IPIA distribution.

α	β	μ'_1	μ'_2	μ'_3	μ'_4	σ^2	ρ_3	ρ_4
0.2	2.8	0.8282	1.0493	8.5982	1857.5528	0.3635	32.526	13868.2
	3.5	0.8418	0.8748	1.6617	43.1078	0.1662	9.5263	1438.03
	4.5	0.863	0.8285	0.9695	2.04	0.0837	4.5394	104.31
	5.5	0.8807	0.8275	0.8596	1.0809	0.0519	3.3445	36.733
0.4	3.5	1.0262	1.3	3.0018	85.9732	0.247	9.4589	1287.58
	4.5	1.0067	1.1275	1.5391	3.7691	0.1139	4.5392	103.66
	5.5	0.999	1.0647	1.2546	1.7893	0.0667	3.3445	36.732
	6.5	0.9955	1.0352	1.1445	1.3936	0.0441	2.8088	23.217
0.6	3.5	1.1522	1.6389	4.2418	128.7299	0.3114	9.4164	1206.31
	4.5	1.1017	1.3501	2.0167	5.3971	0.1364	4.5391	103.266
	5.5	1.0754	1.2339	1.5652	2.403	0.0773	3.3445	36.730
	6.5	1.0596	1.1728	1.3801	1.7886	0.05	2.8088	23.217
0.8	3.5	1.2509	1.9317	5.4209	171.4113	0.367	9.3847	1151.4
	4.5	1.1744	1.5342	2.4431	6.9626	0.1551	4.539	102.97
	5.5	1.1332	1.37	1.8311	2.9623	0.0858	3.3445	36.729
	6.5	1.1076	1.2813	1.576	2.135	0.0546	2.8088	23.217
0.9	3.5	1.2937	2.0662	5.9935	192.7293	0.3925	9.3713	1129.63
	4.5	1.2055	1.6167	2.6426	7.7277	0.1634	4.5389	102.84
	5.5	1.1577	1.4299	1.9526	3.2272	0.0896	3.3445	36.729
	6.5	1.1278	1.3286	1.6641	2.2955	0.0566	2.8088	23.2172
1.2	3.5	1.4045	2.4354	7.6588	256.6091	0.4627	9.3378	1077.91
	4.5	1.2851	1.8372	3.2013	9.9687	0.1857	4.5388	102.535
	5.5	1.2199	1.5876	2.2843	3.9782	0.0995	3.3445	36.728
	6.5	1.1789	1.4516	1.9004	2.7401	0.0619	2.8088	23.217
1.5	3.5	1.497	2.7666	9.2628	320.3961	0.5256	9.3109	1039.23
	4.5	1.3504	2.0287	3.7148	12.1453	0.205	4.5387	102.288
	5.5	1.2704	1.7218	2.58	4.6792	0.1079	3.3445	36.727
	6.5	1.22	1.5548	2.1065	3.1434	0.0663	2.8088	23.217
1.8	3.5	1.577	3.0704	10.8193	384.1067	0.5833	9.2882	1008.5
	4.5	1.4063	2.2	4.1949	14.2718	0.2223	4.5386	102.08
	5.5	1.3132	1.8398	2.8498	5.3426	0.1153	3.3445	36.726
	6.5	1.2547	1.6445	2.2914	3.5166	0.0701	2.8088	23.217

3.3. Moment-Generating Function

The moment generating function (MGF) is an important tool to get moments of distribution and to investigate sums of independent random variables by convolution. The MGF for the IPIA model is represented as:

$$M_W(t) = E\left(e^{tW}\right) = \int_0^\infty e^{tw}\, f(w;\alpha,\beta)\, dw. \tag{10}$$

By applying the exponential series expansion, the expression can be rewritten as follows:

$$M_W(t) = \sum_{r=0}^{\infty} \frac{t^r}{r!} \int_0^\infty w^r\, f(w;\alpha,\beta)\, dw = \sum_{r=0}^{\infty} \frac{t^r}{r!}\, \mu'_r.$$

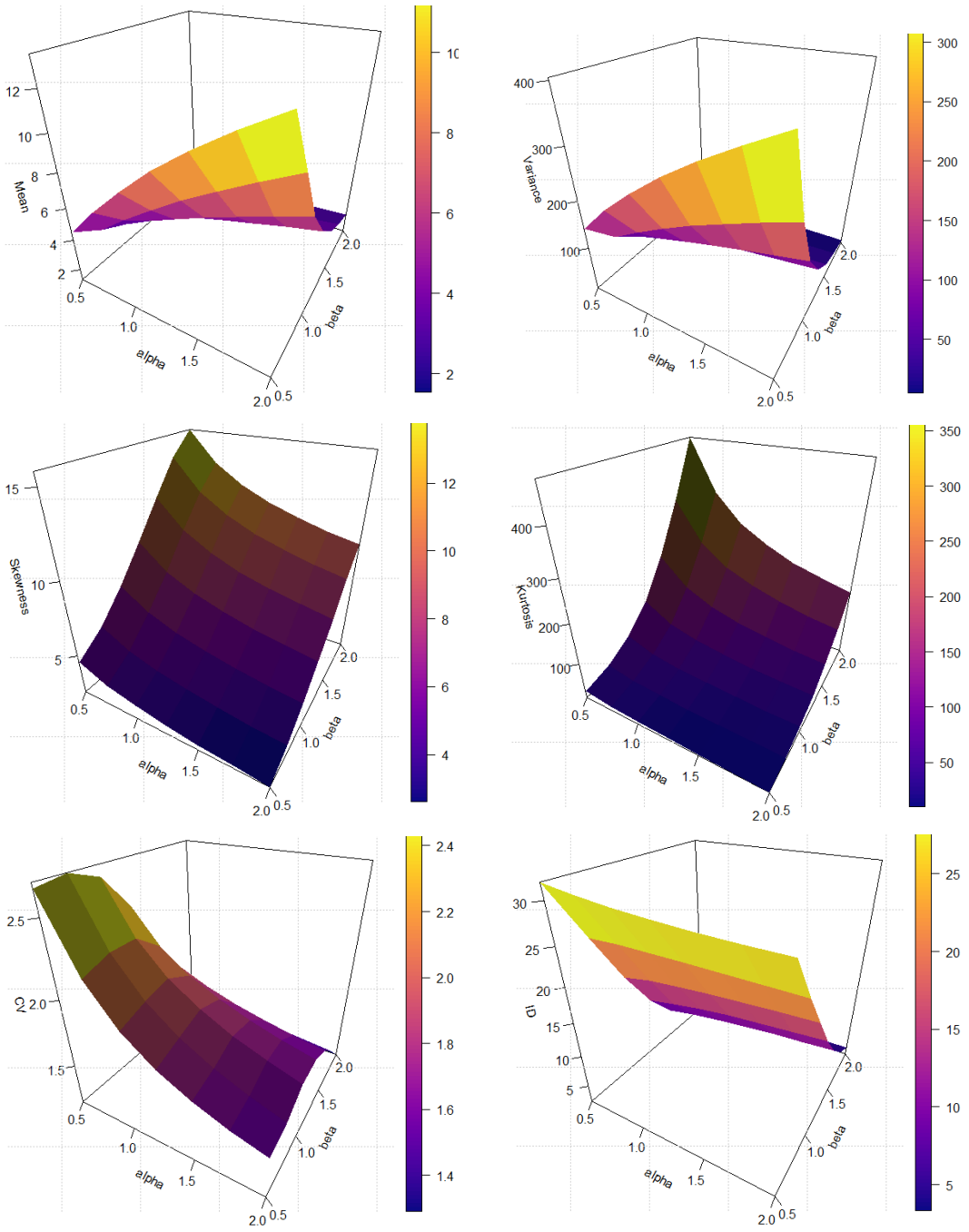


Figure 3. Three-dimensional plots illustrating selected statistical measures of the IPIA distribution.

By applying Eq. (9), the MGF of the IPIA distribution can be expressed as follows:

$$M_W(t) = \sum_{r=0}^{\infty} \frac{t^r}{r!} \frac{1}{2}(2\alpha)^{r/\beta} \left[\Gamma\left(-\frac{r}{\beta}+1\right) + \Gamma\left(-\frac{r}{\beta}+2\right)\right]. \tag{11}$$

3.4. Probability Weighted Moment

The probability weighted moments (PWM) method is a well-established approach for parameter estimation, especially useful when the cumulative distribution function does not have a closed-form inverse. Initially introduced by [28], this technique has found wide application in hydrological and environmental studies. For the IPIA distribution, the general expression of the PWM is given as below:

$$\varphi_{\mathrm{PWM}}(w) = E\left(w^r F^m(w;\alpha,\beta)\right) = \int_0^{\infty} w^r\, F^m(w;\alpha,\beta)\, f(w;\alpha,\beta)\, dw. \tag{12}$$

By substituting Eqs. (3) and (4) into Eq. (12), the following expression for the PWM of the IPIA distribution is obtained:

$$\varphi_{\mathrm{PWM}}(w) = \int_0^{\infty} w^r \left(1+\alpha w^{-\beta}\right)^m \alpha\beta\, w^{-\beta-1} \left(1+2\alpha w^{-\beta}\right) e^{-2(m+1)\alpha w^{-\beta}}\, dw. \tag{13}$$

For any positive real numbers a and b, and for $|\varepsilon| < 1$, the binomial expansion is given by:

$$(a+b)^{\varepsilon} = \sum_{i=0}^{\infty} \binom{\varepsilon}{i} a^{\varepsilon-i} b^i.$$

Consequently, by utilizing this series

$$\left(1+\alpha w^{-\beta}\right)^m = \sum_{k=0}^{m} \binom{m}{k} \alpha^k w^{-k\beta}. \tag{14}$$

By substituting Eq. (14) in Eq. (13), then

$$\varphi_{\mathrm{PWM}}(w) = \sum_{k=0}^{m} \binom{m}{k} \alpha^{k+1} \int_0^{\infty} w^{r-(k+1)\beta-1} \left(1+2\alpha w^{-\beta}\right) e^{-2(m+1)\alpha w^{-\beta}}\, dw. \tag{15}$$

By applying the Gamma function, the PWM of the IPIA distribution can be derived as below:

$$\varphi_{\mathrm{PWM}}(w) = \sum_{k=0}^{m} \binom{m}{k} \frac{(2(m+1)\alpha)^{\frac{r-k\beta}{\beta}}}{2(m+1)} \times \left[\Gamma\left(\frac{-r+k\beta}{\beta}+1\right) + \frac{2\alpha}{(2(m+1)\alpha)^{\frac{-\beta-1}{\beta}}} \Gamma\left(\frac{-r+(k+1)\beta}{\beta}+1\right)\right], \tag{16}$$

where m is a non-negative integer and $r < \beta$ ensures integral convergence.

3.5. Rényi Entropy

The Rényi entropy, introduced by [29], quantifies the degree of uncertainty or randomness within a probability distribution. It is mathematically defined as follows:

$$\begin{aligned} \mathrm{RE}(\eta) &= \frac{1}{1-\eta} \log\left[\int_0^{\infty} f^{\eta}(w)\, dw\right] \\ &= \frac{1}{1-\eta} \log\left[\int_0^{\infty} \left[\alpha\beta\, w^{-\beta-1} \left(1+2\alpha w^{-\beta}\right) e^{-2\alpha w^{-\beta}}\right]^{\eta} dw\right]. \end{aligned} \tag{17}$$

Then, Rényi entropy for the IPIA model is obtained as below:

$$\mathrm{RE}(\eta) = \frac{1}{1-\eta}\log\left[\sum_{j=0}^{\infty}\binom{\eta}{j}\frac{2^j\alpha^{j+\eta}\beta^{\eta}}{(2\eta\alpha)^{\frac{(\eta+j)\beta+\eta}{\beta}}}\Gamma\left(\frac{(\eta+j)\beta+\eta-1}{\beta}\right)\right].$$

3.6. Tsallis Entropy

Tsallis [30] introduced a generalized form of entropy, known as Tsallis entropy, to extend the framework of conventional statistical mechanics. It is mathematically defined as follows:

$$\mathrm{TE}(\eta) = \frac{1}{\eta-1}\log\left[1-\int_0^{\infty} f^{\eta}(w)\,dw\right], \qquad \eta>0,\ \eta\neq 1.$$

Then, Tsallis entropy for the IPIA model is obtained as:

$$\mathrm{TE}(\eta) = \frac{1}{\eta-1}\log\left[1-\sum_{j=0}^{\infty}\binom{\eta}{j}\frac{2^j\alpha^{j+\eta}\beta^{\eta}}{(2\eta\alpha)^{\frac{(\eta+j)\beta+\eta}{\beta}}}\Gamma\left(\frac{(\eta+j)\beta+\eta-1}{\beta}\right)\right].$$

Table 3. Some values of Rényi and Tsallis entropies at different values of parameters.

η	β	α	TE(η)	RE(η)
0.5	0.8	0.5	1.6027	2.4571
		1.5	2.9760	6.8564
		2.5	3.6145	10.1875
	1.2	0.5	0.8976	1.1328
		1.5	1.8131	2.9515
		2.5	2.2388	4.1259
	2	0.5	0.4066	0.4508
		1.5	0.9559	1.2255
		2.5	1.2113	1.6649
0.7	0.8	0.5	0.5289	0.5732
		1.5	1.9022	2.5648
		2.5	2.5407	3.8101
	1.2	0.5	0.3763	0.3983
		1.5	1.2918	1.5778
		2.5	1.7175	2.2468
	2	0.5	0.1189	0.1210
		1.5	0.6682	0.7398
		2.5	0.9236	1.0642
1.5	0.8	0.5	0.3865	0.4264
		1.5	0.9868	0.7789
		2.5	1.6253	1.1126
	1.2	0.5	0.2097	0.2211
		1.5	0.7058	0.5947
		2.5	1.1315	0.8641
	2	0.5	0.2758	0.2957
		1.5	0.2735	0.2556
		2.5	0.5289	0.4648

The flexibility of the model to accommodate multiple structural patterns with different skewness, kurtosis and tail weights is exemplified by these qualities. Thus, the IPIA model provides a very flexible framework for practical use

in many fields of science and engineering. Table 3 presents some numerical values of the Rényi and Tsallis entropies at different parameter values. All computed entropy values are strictly positive and exhibit clear dependence on the model parameters. Moreover, while an increase in the scale parameter (α) leads to higher entropy values, an increase in the shape parameter (β) results in a notable decrease in entropy.

Convergence and monotonicity. The Rényi and Tsallis integral expressions converge if and only if $\eta(\beta+1)>1$. Table 3 has been updated via direct numerical quadrature in R, confirming that Rényi entropy strictly decreases as the entropic order η increases.

4. Methods of Estimation

This section explores some classical approaches for estimating the parameters α and β of the IPIA model. Each technique aims to identify the most suitable parameter estimates by maximizing or minimizing a specific goal function. The considered techniques in this study are the MPS, MLE and BE.

4.1. Maximum Likelihood Estimation

The MLE technique is applied to estimate the parameters of the IPIA distribution. Let $w_1, w_2, \ldots, w_n$ denote a random sample of size n drawn from the IPIA model, representing the observed lifetimes of the studied units. Accordingly, the likelihood function L can be expressed as:

$$L=\prod_{i=1}^{n} f(w_i;\alpha,\beta)=\prod_{i=1}^{n}\alpha\beta\, w_i^{-\beta-1}\left(1+2\alpha w_i^{-\beta}\right)e^{-2\alpha w_i^{-\beta}}.$$

The log-likelihood function, denoted by l, is obtained by taking the natural logarithm of the likelihood function L. It can therefore be expressed as follows

$$\begin{aligned} l&=\sum_{i=1}^{n}\ln f(w_i;\alpha,\beta)=\sum_{i=1}^{n}\ln\left[\alpha\beta\, w_i^{-\beta-1}\left(1+2\alpha w_i^{-\beta}\right)e^{-2\alpha w_i^{-\beta}}\right]\\ &=n\ln(\alpha)+n\ln(\beta)-(\beta+1)\sum_{i=1}^{n}\ln(w_i)+\sum_{i=1}^{n}\ln\left(1+2\alpha w_i^{-\beta}\right)-2\alpha\sum_{i=1}^{n}w_i^{-\beta}. \end{aligned}$$

To determine the MLEs of the parameters α and β, the log-likelihood function is differentiated with respect to each parameter. Setting these partial derivatives to zero yields the following likelihood equations

$$\frac{\partial l}{\partial\alpha}=\frac{n}{\alpha}+\sum_{i=1}^{n}\frac{2w_i^{-\beta}}{1+2\alpha w_i^{-\beta}}-2\sum_{i=1}^{n}w_i^{-\beta}, \tag{18}$$

and

$$\frac{\partial l}{\partial\beta}=\frac{n}{\beta}-\sum_{i=1}^{n}\ln(w_i)-\sum_{i=1}^{n}\frac{2\alpha w_i^{-\beta}\ln(w_i)}{1+2\alpha w_i^{-\beta}}+2\alpha\sum_{i=1}^{n}w_i^{-\beta}\ln(w_i). \tag{19}$$

The MLEs of the unknown parameters can be found by equating Eqs. (18) and (19) to zero. However, due to the nonlinear nature of these equations and the absence of closed-form analytical results, statistical optimization techniques are necessary. In practice, iterative procedures such as the Newton–Raphson algorithm are commonly employed to compute the MLEs efficiently using available computational tools.

The estimators of the parameters, denoted as $\widehat{\alpha}$ and $\widehat{\beta}$, are found by solving the nonlinear likelihood equations derived from the MLE approach. More comprehensive details about this estimation method can be found in Casella and Berger [31]. Also, the necessary specifications for the maximum likelihood estimators are fulfilled for the suggested IPIA model. The estimators therefore possess numerous asymptotic advantages, including consistency, asymptotic normality and asymptotic efficiency. These properties explain the procedure of the MLE approach

for statistical inference and highlight the robustness and reliability of the data analysis carried out in this work, see [43, 44].

Optimization implementation. Numerical optimization was executed via the quasi-Newton BFGS/L-BFGS-B algorithm in R. Analytical gradient vectors were confirmed against finite-difference approximations. Standard errors were derived using the square roots of the diagonal elements of the inverted observed information matrix (Hessian matrix) at convergence.

4.2. Bayesian Estimation

For the BE of the IPIA model, we assume that the parameters α and β have independent prior Gamma distributions, defined as follows:

$$\pi(\alpha) = \alpha^{a_1-1}e^{-b_1\alpha}, \quad \alpha > 0, \qquad \pi(\beta) = \beta^{a_2-1}e^{-b_2\beta}, \quad \beta > 0.$$

The hyperparameters a_i and b_i, for $i = 1, 2$, are meant to be identified and selected to reflect prior principles about the unidentified parameters. The hyperparameters are fixed at $a_1 = a_2 = 0.5$ and $b_1 = b_2 = 0.2$, corresponding to weakly informative Gamma priors. This choice keeps the posterior proper while allowing the likelihood to dominate. This allows one to identify a consistent Bayesian framework for the estimation of the parameters by combining the likelihood function with the prior distributions. The posterior distribution for the parameters α and β is constructed as follows:

$$\pi^*(\alpha, \beta \,|\, w) = \frac{\pi(\alpha)\,\pi(\beta)\,L(\alpha, \beta \,|\, w)}{\int_0^\infty \int_0^\infty \pi(\alpha)\,\pi(\beta)\,L(\alpha, \beta \,|\, w)\,d\alpha\,d\beta}. \tag{20}$$

In this paper, we adopt the squared error loss (SEL) function, which is the most commonly used symmetric loss function in Bayesian inference. As noted in [32], the loss function is a real-valued objective that measures the difference between the estimated and true values of the parameters. The SEL function is defined as:

$$L(\theta - \widehat{\theta}) = (\theta - \widehat{\theta})^2,$$

where $\theta = (\alpha, \beta)$. Under the SEL function, the Bayesian estimator of a parameter minimizes the expected squared deviation between the estimate and the true parameter value. Mathematically, this estimator corresponds to the posterior mean of the parameter, then the BEs under the SEL function are expressed as:

$$\widehat{g}_{BS}(\alpha, \beta \,|\, w) = E_{\alpha,\beta|w}\left(g(\alpha, \beta)\right)$$

and

$$E_{\alpha,\beta}\left(g(\alpha, \beta)\right) = \frac{\int_0^\infty \int_0^\infty g(\alpha, \beta)\,\pi(\alpha)\,\pi(\beta)\,L(\alpha, \beta \,|\, w)\,d\alpha\,d\beta}{\int_0^\infty \int_0^\infty \pi(\alpha)\,\pi(\beta)\,L(\alpha, \beta \,|\, w)\,d\alpha\,d\beta}. \tag{21}$$

It is important to note that the ratio of the integrals in Eq. (21) cannot be expressed in a closed analytical form. Therefore, to obtain samples from the joint posterior distribution in Eq. (21), the Markov Chain Monte Carlo (MCMC) method is employed. Specially, the MCMC procedure is applied utilizing the Gibbs sampler integrated with the Metropolis–Hastings (M–H) algorithm. The joint posterior distribution of the parameters is given by:

$$\pi_1^*(\alpha \,|\, \beta) \propto \alpha^{a_1+n-1}e^{-b_1\alpha}\prod_{i=1}^{n}\left(1 + 2\alpha w_i^{-\beta}\right)e^{-2\alpha w_i^{-\beta}}, \tag{22}$$

and

$$\pi_2^*(\beta \,|\, \alpha) \propto \beta^{a_2+n-1}e^{-b_2\beta}\prod_{i=1}^{n} w_i^{-\beta-1}\left(1 + 2\alpha w_i^{-\beta}\right)e^{-2\alpha w_i^{-\beta}}. \tag{23}$$

The Bayesian estimation of the parameters α and β for the IPIA model is systematically problematic owing to the model's nonlinear construction and characteristic mathematical complication. Obtaining closed-form expressions under the IPIA framework is therefore challenging. To address this limitation, the MCMC approach is adopted as a powerful computational technique for estimating posterior distributions when analytical solutions are not feasible (see Eq. (21)). The conditional posterior distributions of α and β, as indicated by Eqs. (22) and (23), are not part of any standard distribution family. Consequently, the Gibbs sampling procedure is employed, with the Metropolis–Hastings (M–H) algorithm integrated within it to generate samples from the conditional posteriors. The MCMC method constructs a Markov chain whose stationary distribution corresponds to the joint posterior of the parameters, thereby producing a sequence of dependent samples that approximate the target distribution. The generated MCMC samples are subsequently employed to compute posterior summaries, such as posterior means, which serve as the Bayesian estimators of α and β, thereby providing practical estimates of the model parameters based on the posterior distribution. MCMC sampling was conducted using a hybrid Gibbs/Metropolis–Hastings algorithm with Gaussian proposal distributions tuned for an acceptance rate of approximately 30%. Convergence was monitored via effective sample size (ESS > 1000) and trace plots.

4.3. Maximum Product of Spacings Method

Cheng and Amin [33] and Ranneby [34] introduced the MPS method as a reliable alternative to ML estimation. The MPS estimator provides consistent and asymptotically efficient results, especially when ML fails, such as in heavy-tailed or unbounded distributions [35]. Hence, it retains the key advantages of ML while reducing its limitations [36].

The MPS objective function is constructed using all $n+1$ sample spacings

$$D_i(\theta) = F\left(w_{i:n} \,|\, \theta\right) - F\left(w_{i-1:n} \,|\, \theta\right), \qquad i = 1, 2, \ldots, n,$$

where $F\left(w_{0:n} \,|\, \theta\right) = 0$ and $F\left(w_{n+1:n} \,|\, \theta\right) = 1$. Obviously $\sum_{i=1}^{n+1} D_i(\theta) = 1$. In cases of tied observations, a micro-perturbation $\varepsilon = 10^{-7}$ is applied to maintain strictly positive spacing values $D_i(\theta) > 0$ and prevent numerical indefiniteness.

Hence the MPS estimators of the unknown parameter are obtained by maximizing

$$G(\theta) = \left(\prod_{i=1}^{n+1} D_i(\theta)\right)^{\frac{1}{n+1}},$$

or, equivalently, by maximizing the relation:

$$H(\theta) = \frac{1}{n+1} \sum_{i=1}^{n+1} \log D_i(\theta).$$

The MPS estimators for the parameters θ are derived by utilizing numerical methods to resolve the non-linear equation $\partial H(\theta)/\partial\theta = 0$, requiring a numerical solution. The recognized asymptotic equivalence between the ML and the MPS methodologies, as noted in [33], is the basis for the asymptotic confidence intervals for the parameters that are derived by the MPS estimation.

Thus the parameter with MPSE has the following $(1-\gamma)100\%$ confidence interval:

$$\widehat{\theta}_{\mathrm{MPS}} \pm z_{1-\frac{\gamma}{2}} \sqrt{\mathrm{var}\left(\widehat{\theta}_{\mathrm{MPS}}\right)},$$

where $\widehat{\theta}_{\mathrm{MPS}}$ represents the MPS estimators of θ, $z_{1-\frac{\gamma}{2}}$ denotes the percentile of the standard normal distribution, and $\mathrm{var}(\widehat{\theta}_{\mathrm{MPS}})$ signifies the asymptotic variance, calculated using the inverse of the information matrix.

Asymptotic standard errors for MPS are obtained using the inverse of the MPS information matrix. MLE was selected for the primary comparative plots in Section 6 due to its standard comparability with benchmark baseline models.

5. Design of Simulation

This section conducts a rigorous simulation study to evaluate the finite-sample performance and numerical stability of the proposed estimation frameworks. The IPIA distribution is used to generate simulation datasets under different parameter configurations, and the estimation methods described above are applied to estimate the model parameters. We ran $R = 200$ independent Monte Carlo replications for each combination of sample size $n \in \{50, 100, 150, 200\}$ and the five parameter pairs $(\alpha, \beta) \in \{(1.5, 0.5), (2.5, 0.8), (3, 1.2), (3.5, 1.8), (4, 1.5)\}$. This gives a total of $4 \times 5 \times 200 = 4000$ replications. All computations were carried out in R version 4.6.0.

Random samples were generated by drawing $u \sim U(0, 1)$ and evaluating the closed-form quantile function $Q(u)$ in Eq. (7) directly; no numerical inversion is required. The branch W_{-1} is used. We verified numerically that $F(Q(u)) = u$ for $u \in (0, 1)$.

For the MPS method, 95% confidence intervals were obtained using $B = 300$ parametric bootstrap resamples. For the Bayesian method, we used 5000 MCMC draws after a burn-in of 1000. Nonconvergent replications were discarded.

(i) $R = 200$ independent Monte Carlo replications are used to compute RBIAS, MSE, CP, and AW.
(ii) $B = 300$ parametric bootstrap resamples are used only to construct the MPS confidence intervals within each replication.
(iii) 5000 MCMC draws after a 1000-iteration burn-in are used only to compute the Bayesian posterior means within each replication.

The results are reported in Tables 4-13. The main findings are summarized as follows:

- The minimal values of RBIAS and MSEs recorded for both α and β parameters indicate that all three estimation methods exhibit consistent performance across varying sample sizes.
- The MSEs of all estimation methods decrease with the increase of sample size, which indicates the better precision of parameters estimation with a larger data set.
- In general, as sample sizes increase, the RBIAS diminishes, signifying that estimators have reduced bias.
- MLE and BE have similar MSEs and RBIAS values, with MLE demonstrating a marginal advantage, particularly for smaller sample sizes; however, both approaches are effective generally.
- Confidence intervals AWs are decreasing with the increase of sample size for all estimation techniques, which implies that the estimations are more precise with larger datasets.

Table 4. Outcomes of point estimating techniques for the IPIA model at $\alpha = 1.5$ and $\beta = 0.5$.

		α			β		
n	Methods	Mean	MSEs	RBIAS	Mean	MSEs	RBIAS
50	MLE	1.5591	0.0521	0.0394	0.5117	0.0036	0.0235
	BE	1.5599	0.0528	0.0399	0.5138	0.0037	0.0277
	MPSE	1.4762	0.0385	0.0159	0.4766	0.0036	0.0468
100	MLE	1.5239	0.0181	0.0159	0.5099	0.0018	0.0198
	BE	1.5234	0.0183	0.0156	0.5108	0.0019	0.0215
	MPSE	1.4777	0.0156	0.0148	0.489	0.0017	0.0221
150	MLE	1.5137	0.0145	0.0091	0.5087	0.0013	0.0174
	BE	1.5129	0.0143	0.0086	0.5092	0.0013	0.0176
	MPSE	1.4801	0.0133	0.0133	0.4931	0.0012	0.0137
200	MLE	1.5115	0.0112	0.0077	0.5062	0.0008	0.0125
	BE	1.5119	0.0113	0.0079	0.5066	0.0008	0.0133
	MPSE	1.4847	0.0103	0.0102	0.4938	0.0008	0.0124

Table 5. Outcomes of point estimating techniques for the IPIA model at $\alpha = 2.5$ and $\beta = 0.8$.

		α			β		
n	Methods	Mean	MSEs	RBIAS	Mean	MSEs	RBIAS
50	MLE	2.6413	0.2289	0.0565	0.8188	0.0093	0.0235
	BE	2.6443	0.2299	0.0577	0.8204	0.0092	0.0255
	MPSE	2.4112	0.1583	0.0355	0.7626	0.0090	0.0468
100	MLE	2.5699	0.0782	0.028	0.8158	0.0046	0.0198
	BE	2.5698	0.0806	0.0279	0.8166	0.0048	0.0207
	MPSE	2.4393	0.0646	0.0243	0.7824	0.0044	0.022
150	MLE	2.5484	0.0589	0.0193	0.8139	0.0034	0.0174
	BE	2.5469	0.0583	0.0188	0.8141	0.0034	0.0176
	MPSE	2.4521	0.0517	0.0191	0.789	0.0031	0.0137
200	MLE	2.537	0.0413	0.0148	0.81	0.0021	0.0125
	BE	2.5379	0.0413	0.0151	0.8103	0.0021	0.0128
	MPSE	2.4603	0.0372	0.0159	0.7901	0.0020	0.0124

Table 6. Outcomes of point estimating techniques for the IPIA model at $\alpha = 3$ and $\beta = 1.2$.

		α			β		
n	Methods	Mean	MSEs	RBIAS	Mean	MSEs	RBIAS
50	MLE	3.1911	0.4009	0.0637	1.2281	0.0208	0.0234
	BE	3.1872	0.3884	0.0623	1.2274	0.0201	0.0228
	MPSE	2.8751	0.2705	0.0416	1.1438	0.0205	0.0467
100	MLE	3.0983	0.1376	0.0327	1.2237	0.0104	0.0197
	BE	3.0957	0.1401	0.0318	1.2231	0.0105	0.0192
	MPSE	2.9183	0.1115	0.0272	1.1736	0.0098	0.0219
150	MLE	3.0699	0.1014	0.0233	1.2209	0.0076	0.0174
	BE	3.0663	0.0993	0.0221	1.2201	0.0075	0.0167
	MPSE	2.9372	0.0872	0.0209	1.1835	0.0071	0.0137
200	MLE	3.0526	0.0689	0.0175	1.2149	0.0046	0.0124
	BE	3.0531	0.0687	0.0177	1.2148	0.0045	0.0123
	MPSE	2.9469	0.0611	0.0176	1.1851	0.0044	0.0124

Table 7. Outcomes of point estimating techniques for the IPIA model at $\alpha = 3.5$ and $\beta = 1.8$.

		α			β		
n	Methods	Mean	MSEs	RBIAS	Mean	MSEs	RBIAS
50	MLE	3.7458	0.6462	0.0702	1.8423	0.0471	0.0235
	BE	3.7218	0.5939	0.0634	1.8339	0.0436	0.0189
	MPSE	3.3374	0.4264	0.0465	1.7158	0.0464	0.0468
100	MLE	3.6297	0.2226	0.0371	1.8356	0.0235	0.0198
	BE	3.6209	0.2223	0.0345	1.8317	0.0232	0.0176
	MPSE	3.3966	0.1771	0.0295	1.7605	0.0221	0.0219
150	MLE	3.5939	0.1611	0.0268	1.8314	0.0171	0.0174
	BE	3.5851	0.1553	0.0243	1.8282	0.0167	0.0157
	MPSE	3.4219	0.1364	0.0223	1.7753	0.0158	0.0137
200	MLE	3.5698	0.1071	0.0199	1.8225	0.0104	0.0125
	BE	3.5677	0.1053	0.0193	1.8209	0.0102	0.0117
	MPSE	3.4329	0.0939	0.0192	1.7776	0.0099	0.0124

Table 8. Outcomes of point estimating techniques for the IPIA model at $\alpha = 4$ and $\beta = 1.5$.

		α			β		
n	Methods	Mean	MSEs	RBIAS	Mean	MSEs	RBIAS
50	MLE	4.3049	0.9767	0.0762	1.5352	0.0326	0.0235
	BE	4.2668	0.8649	0.0667	1.5259	0.0294	0.0173
	MPSE	3.7985	0.6315	0.0504	1.4298	0.0322	0.0468
100	MLE	4.1636	0.3372	0.0409	1.5296	0.0163	0.0198
	BE	4.1452	0.3312	0.0363	1.5245	0.0159	0.0163
	MPSE	3.8743	0.2639	0.0314	1.4671	0.0154	0.0220
150	MLE	4.1201	0.2407	0.0301	1.5261	0.0119	0.0174
	BE	4.1074	0.2299	0.0269	1.5229	0.0114	0.0152
	MPSE	3.9064	0.2009	0.0234	1.4794	0.0110	0.0137
200	MLE	4.0885	0.1572	0.0221	1.5187	0.0072	0.0125
	BE	4.0841	0.1547	0.0210	1.5171	0.0072	0.0114
	MPSE	3.9185	0.1366	0.0204	1.4814	0.0069	0.0124

Table 9. Outcomes of interval estimate techniques for the IPIA model at $\alpha = 1.5$ and $\beta = 0.5$.

		α				β			
n	Methods	Lower	Upper	CPs	AWs	Lower	Upper	CPs	AWs
50	MLE	1.2097	2.0096	0.920	0.7999	0.4089	0.6404	0.935	0.2315
	BE	1.1776	1.956	0.910	0.7784	0.4024	0.6291	0.935	0.2267
	MPSE	1.1419	1.8514	0.895	0.7096	0.3654	0.573	0.860	0.2077
100	MLE	1.2763	1.8195	0.955	0.5433	0.4352	0.5974	0.945	0.1622
	BE	1.2616	1.793	0.955	0.5314	0.4315	0.5912	0.940	0.1597
	MPSE	1.2311	1.7296	0.950	0.4985	0.4066	0.5565	0.905	0.1499
150	MLE	1.3101	1.749	0.935	0.4389	0.4472	0.5787	0.945	0.1315
	BE	1.3021	1.7316	0.935	0.4294	0.4449	0.5746	0.940	0.1297
	MPSE	1.2747	1.683	0.910	0.4083	0.4256	0.549	0.885	0.1234
200	MLE	1.3340	1.7127	0.945	0.3788	0.4528	0.566	0.955	0.1132
	BE	1.3290	1.6997	0.935	0.3707	0.4513	0.5626	0.965	0.1114
	MPSE	1.3027	1.6617	0.910	0.359	0.4346	0.5426	0.920	0.1081

Table 10. Outcomes of interval estimate techniques for the IPIA model at $\alpha = 2.5$ and $\beta = 0.8$.

		α				β			
n	Methods	Lower	Upper	CPs	AWs	Lower	Upper	CPs	AWs
50	MLE	1.9441	3.5910	0.930	1.647	0.6543	1.0247	0.935	0.3704
	BE	1.8751	3.4510	0.935	1.5759	0.6419	1.0038	0.950	0.3619
	MPSE	1.7726	3.1489	0.880	1.3763	0.5846	0.9168	0.860	0.3323
100	MLE	2.0782	3.1784	0.970	1.1003	0.6963	0.9558	0.945	0.2595
	BE	2.0467	3.1141	0.975	1.0674	0.69	0.9448	0.945	0.2548
	MPSE	1.9582	2.9275	0.945	0.9694	0.6505	0.8903	0.905	0.2398
150	MLE	2.1447	3.0281	0.965	0.8834	0.7155	0.926	0.925	0.2105
	BE	2.1244	2.983	0.950	0.8586	0.7114	0.9183	0.925	0.2069
	MPSE	2.0482	2.8440	0.905	0.7959	0.681	0.8784	0.885	0.1974
200	MLE	2.1862	2.9442	0.955	0.7581	0.7245	0.9056	0.955	0.1811
	BE	2.1725	2.9111	0.955	0.7386	0.7228	0.8999	0.955	0.1771
	MPSE	2.1034	2.8003	0.905	0.6969	0.6954	0.8682	0.920	0.1729

Table 11. Outcomes of interval estimate techniques for the IPIA model at $\alpha = 3$ and $\beta = 1.2$.

		α				β			
n	Methods	Lower	Upper	CPs	AWs	Lower	Upper	CPs	AWs
50	MLE	2.2851	4.4607	0.935	2.1756	0.9814	1.537	0.935	0.5556
	BE	2.1936	4.2538	0.925	2.0602	0.9603	1.5002	0.940	0.5399
	MPSE	2.057	3.8371	0.87	1.7801	0.9758	1.3355	0.905	0.3598
100	MLE	2.4592	3.9042	0.965	1.445	1.0445	1.4337	0.945	0.3892
	BE	2.4119	3.8057	0.965	1.3939	1.0342	1.4147	0.930	0.3805
	MPSE	2.2979	3.5546	0.94	1.2568	1.001	1.326	0.900	0.3250
150	MLE	2.5454	3.703	0.96	1.1575	1.0732	1.3889	0.925	0.3157
	BE	2.5119	3.6405	0.95	1.1286	1.0667	1.3761	0.925	0.3095
	MPSE	2.4148	3.4461	0.895	1.0313	1.0214	1.3175	0.885	0.2961
200	MLE	2.5971	3.5882	0.955	0.9911	1.0867	1.3584	0.955	0.2717
	BE	2.5797	3.5461	0.96	0.9664	1.0835	1.3488	0.950	0.2653
	MPSE	2.4845	3.3871	0.92	0.9026	1.043	1.3023	0.920	0.2593

Table 12. Outcomes of interval estimate techniques for the IPIA model at $\alpha = 3.5$ and $\beta = 1.8$.

		α				β			
n	Methods	Lower	Upper	CPs	AWs	Lower	Upper	CPs	AWs
50	MLE	2.6068	5.3621	0.935	2.7753	1.4541	2.2805	0.935	0.8265
	BE	2.4839	5.0561	0.945	2.5721	1.4384	2.2398	0.945	0.8015
	MPSE	2.3296	4.5447	0.880	2.2152	1.3153	2.0629	0.860	0.7476
100	MLE	2.8261	4.6471	0.960	1.8211	1.5573	2.1386	0.935	0.5813
	BE	2.7679	4.5183	0.955	1.7503	1.5472	2.1176	0.930	0.5704
	MPSE	2.6255	4.1947	0.930	1.5692	1.4636	2.0032	0.905	0.5396
150	MLE	2.9345	4.3911	0.960	1.4565	1.6033	2.0756	0.930	0.4722
	BE	2.8949	4.3042	0.950	1.4093	1.5991	2.0621	0.920	0.4629
	MPSE	2.7715	4.0582	0.895	1.2867	1.5322	1.9763	0.885	0.4441
200	MLE	2.9979	4.2427	0.960	1.2448	1.6251	2.0318	0.955	0.4066
	BE	2.9785	4.1839	0.960	1.2053	1.6251	2.0215	0.970	0.3964
	MPSE	2.8565	3.9843	0.915	1.1278	1.5645	1.9535	0.920	0.3889

Table 13. Outcomes of interval estimate techniques for the IPIA model at $\alpha = 4$ and $\beta = 1.5$.

		α				β			
n	Methods	Lower	Upper	CPs	AWs	Lower	Upper	CPs	AWs
50	MLE	2.9312	6.3247	0.935	3.3935	1.2117	1.9004	0.935	0.6887
	BE	2.7693	5.9050	0.950	3.1356	1.1967	1.8650	0.945	0.6683
	MPSE	2.5914	5.2747	0.870	2.6833	1.0961	1.7191	0.860	0.6230
100	MLE	3.1926	5.4229	0.950	2.2302	1.2977	1.7822	0.935	0.4844
	BE	3.1164	5.2390	0.960	2.1226	1.2902	1.7632	0.945	0.4730
	MPSE	2.9448	4.8451	0.920	1.9003	1.2197	1.6694	0.905	0.4497
150	MLE	3.3226	5.1028	0.955	1.7802	1.3361	1.7296	0.930	0.3935
	BE	3.2689	4.9821	0.970	1.7132	1.3312	1.7172	0.925	0.3860
	MPSE	3.1207	4.6812	0.895	1.5605	1.2768	1.6469	0.886	0.3701
200	MLE	3.3970	4.9155	0.950	1.5185	1.3543	1.6931	0.955	0.3388
	BE	3.3629	4.8347	0.950	1.4718	1.3523	1.6835	0.960	0.3313
	MPSE	3.2222	4.5901	0.915	1.3680	1.3038	1.6279	0.920	0.3241

6. Data Analysis

In order to fully test the IPIA model against real-world complexities, the model was applied to two different datasets taken from completely different fields of knowledge. We estimate parameters using the maximum likelihood estimator (MLE) because of its well-known asymptotic properties and perform all numerical analyses in the R 4.6.0 environment to ensure full transparency and reproducibility. We assess the fitting efficacy of the IPIA model in comparison to several rival models, namely: the induced Ailamujia (IAL), generalized exponential (GEx), Weibull (We), Gamma (Ga), and entropy Chen (EC) [37] distributions. We have applied several model selection criteria and goodness-of-fit statistics using classical methods. For model selection, we utilized the Akaike Information Criterion (AIC), Bayesian Information Criterion (BIC), Corrected Akaike Information Criterion (CAIC), and Hannan–Quinn Information Criterion (HQIC). Also, we employed the Kolmogorov–Smirnov (K-S) test statistic for the goodness-of-fit evaluation, accompanied by the corresponding p-value. Additionally, the fitted distributions were compared using the Cramér–von Mises (CVM) and the Anderson–Darling (AD) tests. The distribution with the lowest values of AIC, BIC, CAIC, HQIC, K-S, CVM, AD and the highest p-value is the superior fit. Both datasets were divided by 10 before fitting to improve numerical stability and ensure a good model fit. This rescaling does not affect the model comparison, since it shifts the maximized log-likelihood equally for every model and leaves the fitted CDF values unchanged. The MLE is used for the real-data analysis because it is the method with the established asymptotic properties required for the information criteria and goodness-of-fit statistics, because it is the method used by all competing models, and because it provides standard errors and confidence intervals directly.

6.1. Data Set I

The first dataset comprises the active repair times (in hours) for aerial communication transceivers, as studied by Lemonte *et al.* [38]. The information is as follows: 0.5, 0.6, 3, 3, 0.6, 1, 1, 0.7, 0.7, 0.7, 0.8, 0.8, 1, 1, 1.1, 1.3, 1.5, 1.5, 2, 2, 2.2, 2.5, 2.7, 3.3, 4, 1.5, 1.5, 4, 4.5, 4.7, 5, 5.4, 5.4, 7, 7.5, 8.8, 9, 10.2, 22, 24.5. The data is examined using several descriptive statistics presented in Table 14. Figure 4 depicts the visual representations of the dataset. The histogram and kernel density plots depict the empirical distribution and its smooth approximation, highlighting the concentration of the majority of observations at lower values. The boxplot and violin plot validate the existence of right skewness and several outlier findings. The TTT plot demonstrates a declining failure rate trend, whilst the Q–Q plot displays a satisfactory alignment between the empirical and theoretical quantiles, so validating the suggested model's appropriateness.

Table 15 displays the MLEs of the parameters, with their standard errors for each distribution. From the results of Table 16, we conclude that the IPIA distribution offers the most suitable fit, evidenced by its minimal values of AIC, BIC, CAIC, HQIC, K-S, CVM, AD, alongside the maximal p-value. The IPIA distribution provides the best fit among the models considered for this dataset, although the differences with some competitors are modest. Figure 5 depicts some fitted graphical plots, including the estimated PDF, empirical CDF, and P-P plots of the competing models, indicating that our distribution closely corresponds with the supplied dataset.

Table 14. Some statistics measures for the repair times dataset.

Dataset	n	Mean	Median	Variance	Skewness	Kurtosis	Range	Min	Max
I	40	4.0125	2.1	26.6801	2.7171	10.5433	24	0.5	24.5

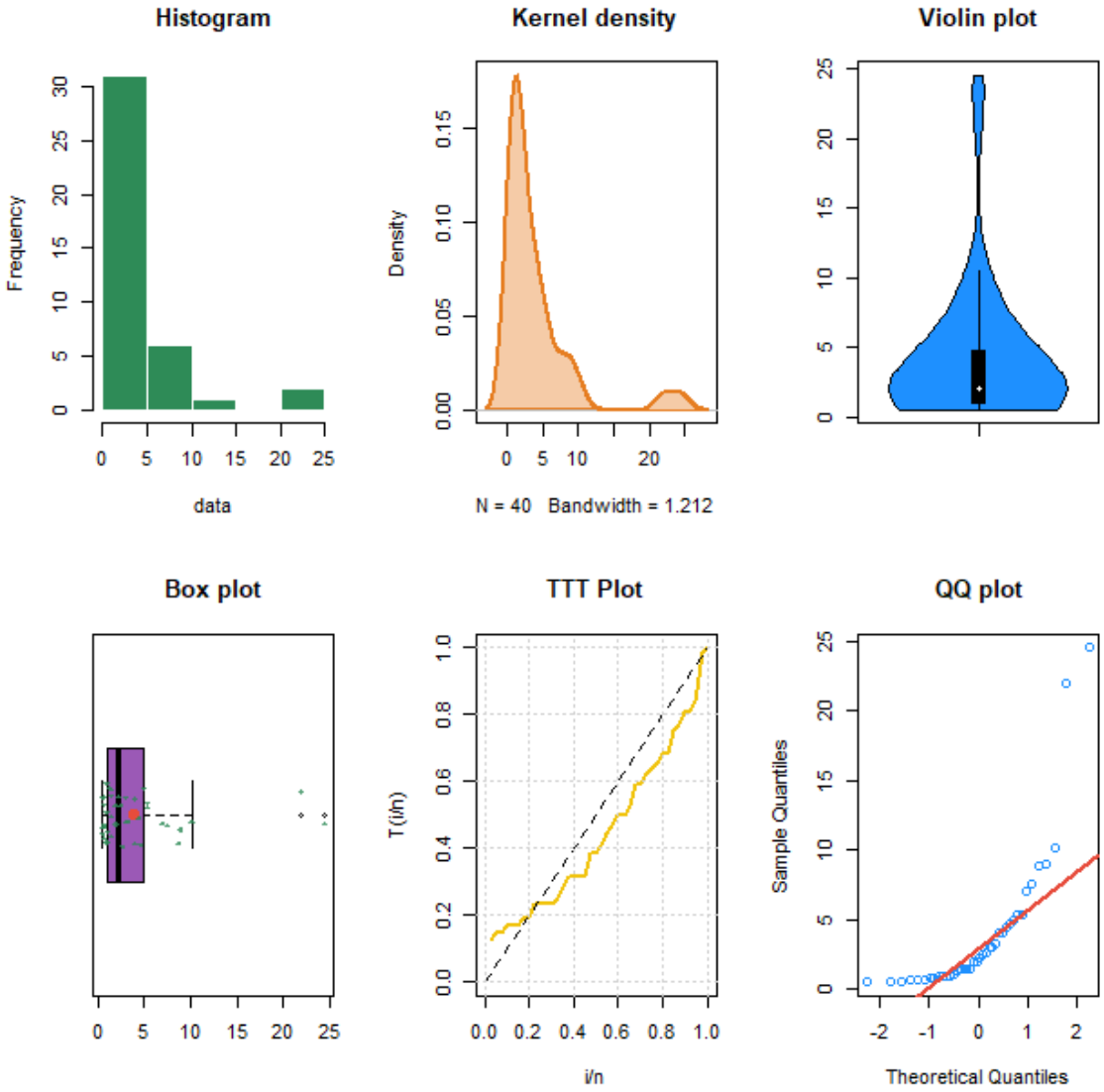


Figure 4. Some non-parametric plots for the repair times dataset.

Table 15. MLEs with its standard errors of the parameters for the repair times dataset

Models	$\hat{\alpha}$	SE($\hat{\alpha}$)	$\hat{\beta}$	SE($\hat{\beta}$)
IPIA	1.1631	0.1618	1.0764	0.1397
IAL	0.1822	0.0256	–	–
Ga	1.0617	0.2101	0.3781	0.0947
We	0.9607	0.1089	3.9282	0.6872
GEx	1.1132	0.2444	3.7359	0.7822
EC	0.5731	0.0852	0.3142	0.0259

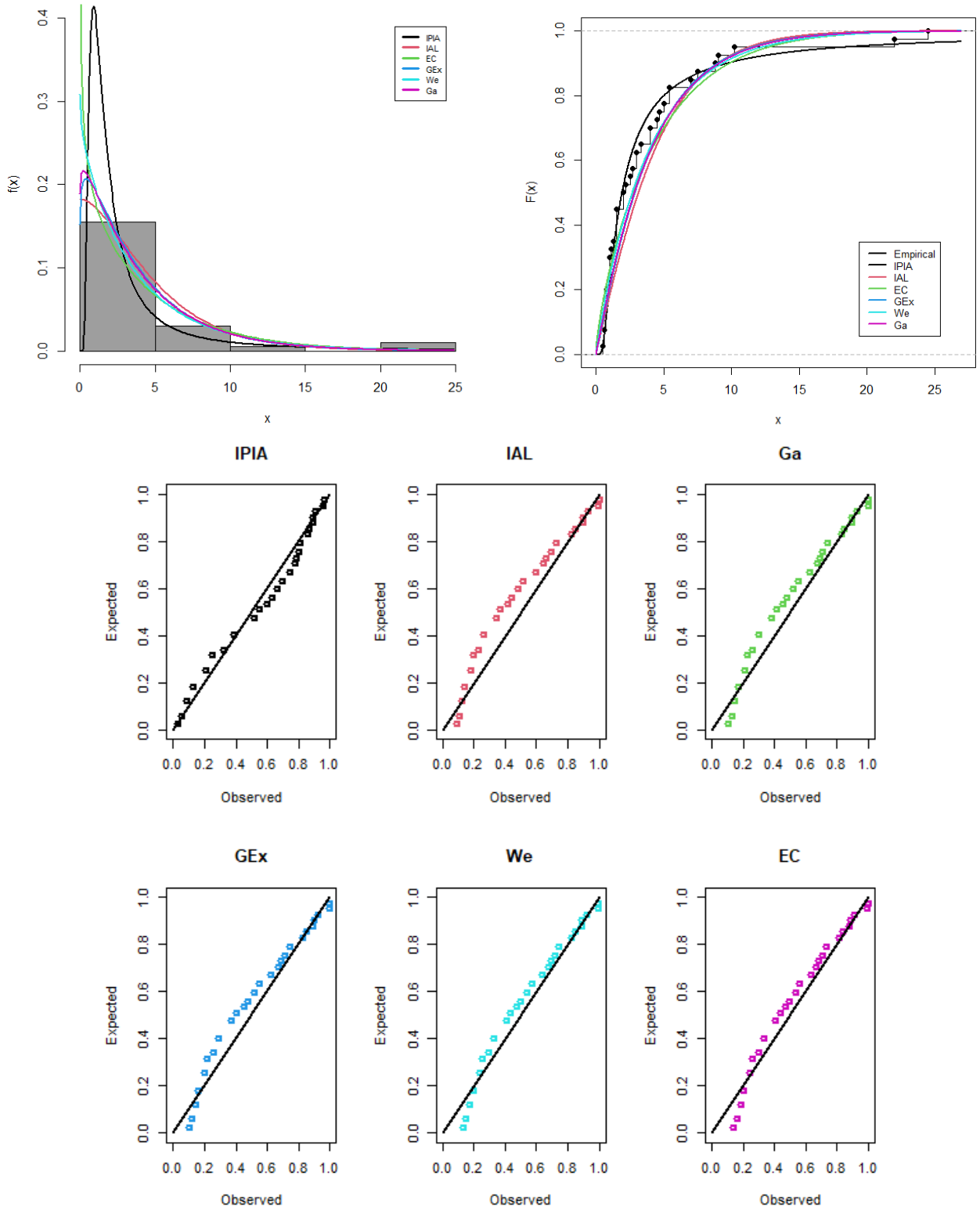


Figure 5. Graphical representation of some plots for the repair times dataset.

Table 16. Some goodness of fit measures for the repair times dataset

Models	AIC	BIC	CAIC	HQIC	K–S	P-value	CVM	AD
IPIA	183.34	186.72	183.66	184.56	0.098	0.839	0.074	0.452
IAL	196.68	198.37	196.79	197.29	0.187	0.121	0.315	1.844
Ga	195.06	198.44	195.39	196.28	0.151	0.324	0.178	1.173
We	195.02	198.41	195.35	196.24	0.129	0.518	0.136	1.021
GEx	194.92	198.29	195.24	196.14	0.158	0.269	0.191	1.224
EC	199.19	202.57	199.51	200.41	0.139	0.425	0.153	1.153

6.2. Data Set II

The second data set is the monthly actual taxes income in Egypt from January 2006 to November 2010, studied by [39]. The data (in 1000 million Egyptian pounds) is provided as follows: 6.8, 17, 11, 12.5, 8.4, 5.2, 5.9, 20.4, 14.9, 21.3, 16.2, 17.2, 7.8, 6.1, 9.2, 10.2, 11.9, 8.5, 9.6, 13.3, 8.5, 21.6, 18.5, 7.1, 5.1, 6.7, 8.6, 9.7, 39.2, 35.7, 11.6, 15.7, 9.7, 8.9, 10, 10.8, 4.1, 36.0, 8.5, 8.0, 9.2, 26.2, 21.9, 16.7, 35.4, 14.3, 10.6, 6.1, 19.1, 20.5, 7.1, 7.7, 18.1, 16.5, 11.9, 7, 8.6, 10.3, 11.2. Table 17 displays a few descriptive measures of the data. Figure 6 depicts the graphical representations of the dataset via several diagnostic plots. The histogram and kernel density plots illustrate the empirical distribution and its smooth estimation, demonstrating that the majority of observations are concentrated at lower values. The violin and box plots further verify the existence of right skewness and several outliers. The TTT plot reveals a diminishing failure trend, suggesting that reliability enhances gradually over time. The Q–Q figure demonstrates a robust correlation between the observed and expected quantiles, reinforcing the notion that our proposed model sufficiently accommodates the data, exhibiting no significant deviations from the anticipated distribution.

Table 18 presents the MLEs of the parameters, together with their standard errors for each distribution. Table 19 shows that the IPIA model attains the smallest values of the information criteria and goodness-of-fit statistics AIC, BIC, CAIC, HQIC, K-S, CVM, AD, and the greatest p-value. Consequently, these results suggest that the IPIA provides a better fit than the competing models for this dataset. Visualizations in Figure 7, encompassing the estimated PDF, empirical CDF, and P-P plots across the fitted models, further substantiate this. The near-perfect alignment between the empirical and theoretical curves demonstrates that the proposed IPIA distribution captures the characteristics of this real-world dataset most accurately.

Table 17. Some statistics measures for the taxes income dataset.

Dataset	n	Mean	Median	Variance	Skewness	Kurtosis	Range	Min	Max
II	59	13.4881	10.6	64.8266	1.6083	5.2560	35.1	4.1	39.2

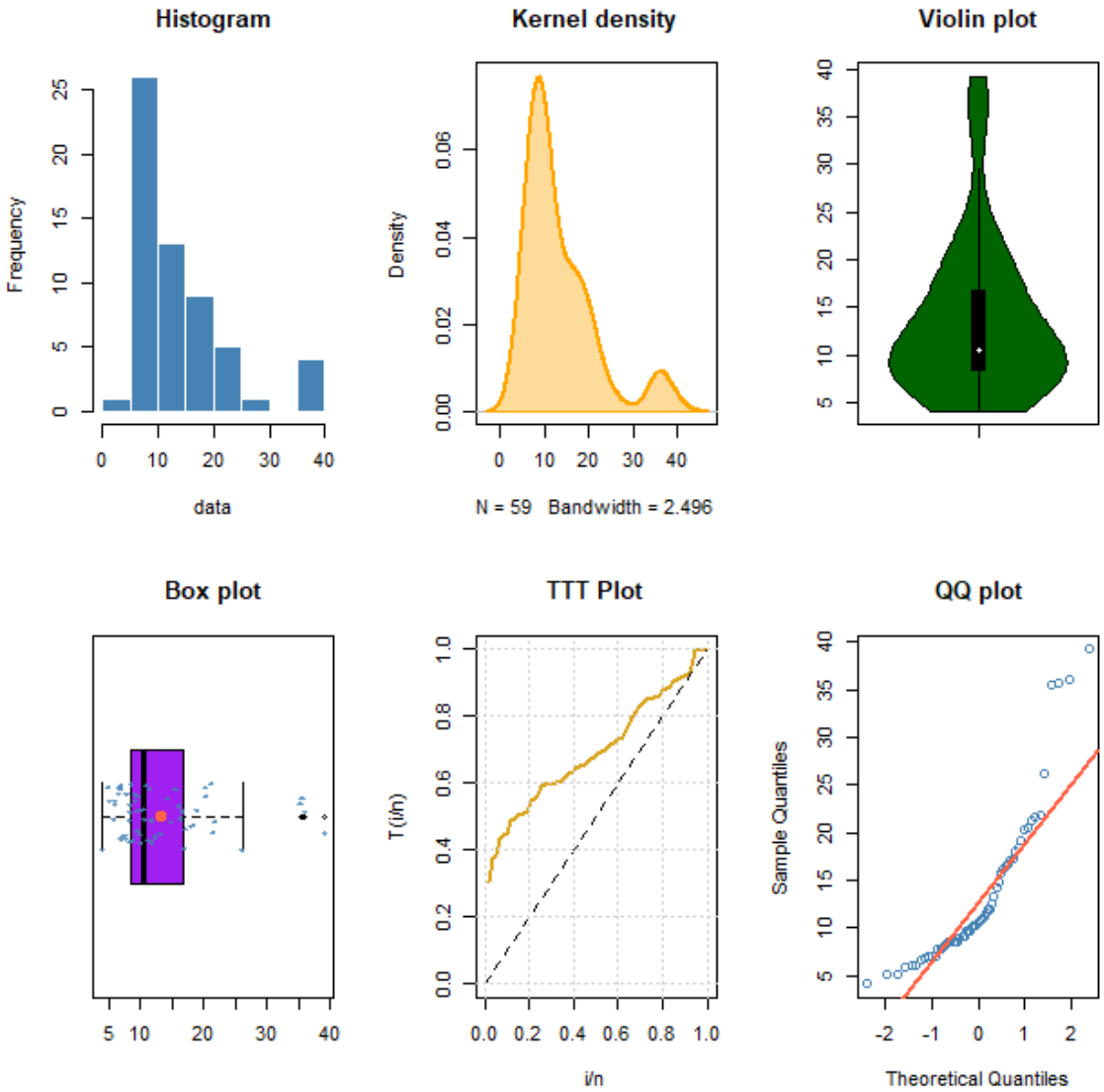


Figure 6. Some non-parametric plots for the taxes income dataset.

Table 18. MLEs with its standard errors of the parameters for the taxes income dataset

Models	$\hat{\alpha}$	SE($\hat{\alpha}$)	$\hat{\beta}$	SE($\hat{\beta}$)
IPIA	65.023	27.395	1.9953	0.2031
IAL	0.0582	0.0065	–	–
Ga	3.6788	0.6491	3.6665	0.6932
We	1.8395	0.1711	15.3047	1.1516
GEx	5.5331	1.4339	5.5946	0.7283
EC	0.1194	0.0239	0.3929	0.0184

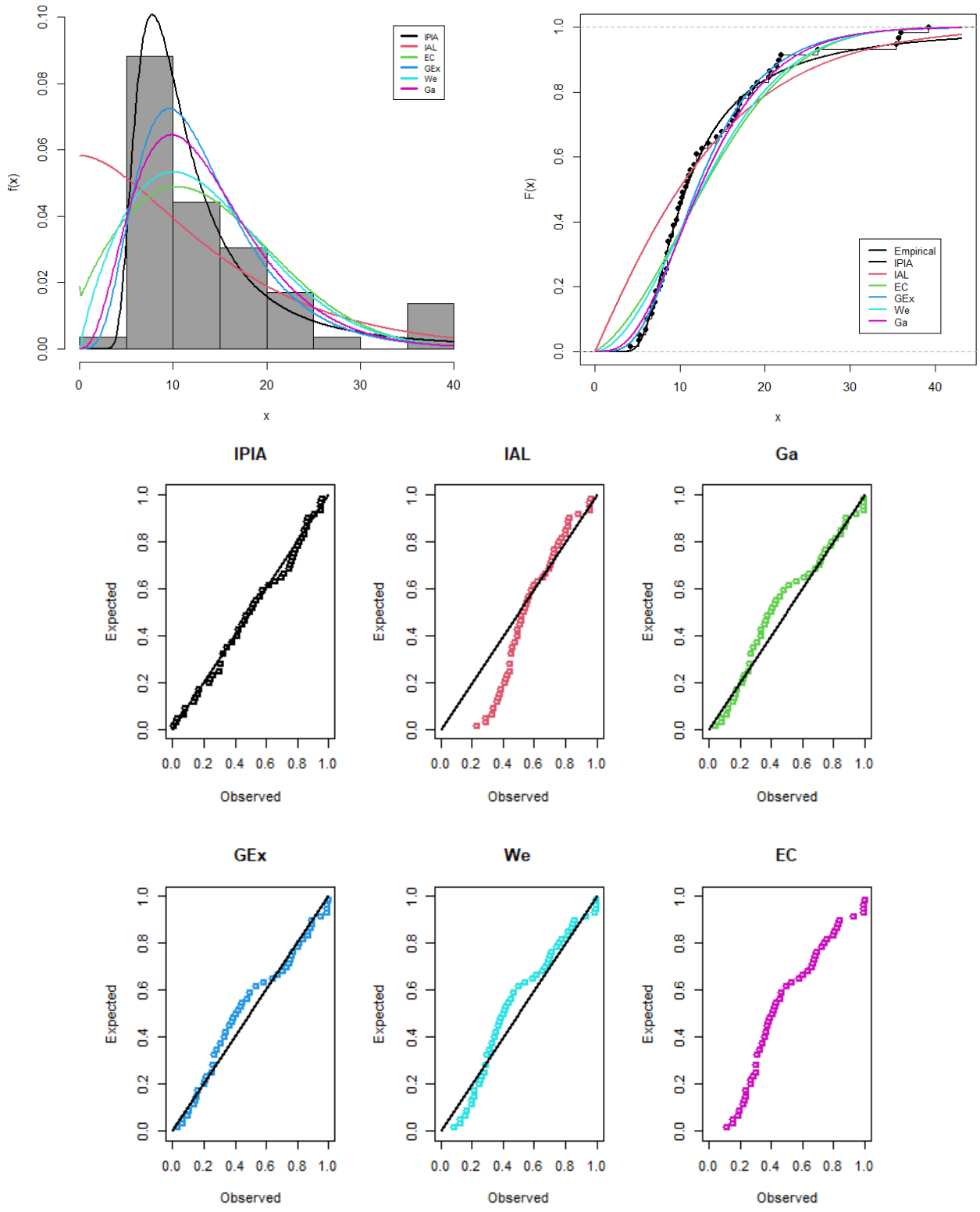


Figure 7. Graphical representation of some plots for the taxes income dataset.

Table 19. Some goodness of fit measures for the taxes income dataset

Models	AIC	BIC	CAIC	HQIC	K–S	P-value	CVM	AD
IPIA	382.58	386.74	382.79	384.21	0.065	0.966	0.035	0.276
IAL	417.72	419.81	417.79	418.53	0.273	0.009	1.012	3.525
Ga	390.16	394.32	390.38	391.79	0.134	0.243	0.203	1.230
We	398.58	402.74	398.79	400.21	0.143	0.178	0.281	1.741
GEx	386.45	390.61	386.66	388.07	0.115	0.419	0.157	0.942
EC	404.27	408.42	404.48	405.89	0.144	0.175	0.352	2.341

7. Conclusion

This study introduces a novel distribution known as the inverse power induced Ailamujia (IPIA) distribution, defined by two parameters that extend the scope of the induced Ailamujia distribution. Several statistical properties of the proposed distribution were derived, including its survival and hazard rate functions, quantile function, raw moments, moment-generating function, and probability-weighted moments, along with summary measures such as the mean, variance, skewness, and kurtosis. Furthermore, both Rényi and Tsallis entropies were evaluated. To estimate the parameters of the IPIA model, three distinct approaches were employed: maximum likelihood estimation (MLE), maximum product of spacings (MPS), and Bayesian estimation (BE). Finally, the performance and accuracy of these estimation methods were validated through a comprehensive Monte Carlo simulation study. The importance of the model related with the IPIA is demonstrated by two applications of biomedical and industrial datasets, in connection to various contemporary statistical distributions. Our framework is not limited to the current analysis and can be extended in various relevant ways. For example, it can be applied to censored or abridged data and its utility can be further explored within the framework of reliability engineering and risk assessment. All these possible paths make the IPIA model an exciting prospect for further research and practical implementation.

Acknowledgement

The authors extend their appreciation to Umm Al-Qura University, Saudi Arabia for funding this research work through grant number: 26UQU4340119GSSR05.

Funding

This research work was funded by Umm Al-Qura University, Saudi Arabia under grant number: 26UQU4340119GSSR05.

Conflicts of Interest

The authors declare no conflicts of interest.

REFERENCES

1. V. K. Sharma, S. K. Singh, and U. Singh, *A new upside-down bathtub shaped hazard rate model for survival data analysis*, Applied Mathematics and Computation, vol. 239, no. 15, pp. 242–253, 2014. doi:10.1016/j.amc.2014.04.048
2. C. Chesneau, and V. Agiwal, *Statistical theory and practice of the inverse power Muth distribution*, Journal of Computational Mathematics and Data Science, vol. 1, Article 100004, 2021. doi:10.1016/j.jcmds.2021.100004

3. K. V. P. Barco, J. Mazucheli, and V. Janeiro, *The inverse power Lindley distribution*, Communications in Statistics - Simulation and Computation, vol. 46, no. 8, pp. 6308–6323, 2017. doi:10.1080/03610918.2016.1202274
4. A. M. Abd AL-Fattah, A. A. El-Helbawy, and G. R. Al-Dayian, *Inverted Kumaraswamy distribution: Properties and estimation*, Pakistan Journal of Statistics, vol. 33, no. 1, pp. 37–61, 2017.
5. A. S. Hassan, and R. E. Mohammed, *Parameter estimation of inverse exponentiated Lomax distribution with right censored data*, Gazi University Journal of Science, vol. 32, no. 4, pp. 1370–1386, 2019. doi:10.35378/gujs.471676
6. M. H. Tahir, G. M. Cordeiro, S. Ali, S. Dey, and A. Manzoor, *The inverted Nadarajah-Haghighi distribution: estimation methods and applications*, Journal of Statistical Computation and Simulation, vol. 88, no. 14, pp. 2775–2798, 2018. doi:10.1080/03610918.2018.1441416
7. A. S. Hassan, M. Elgarhy, and R. Ragab, *Statistical properties and estimation of inverted Topp-Leone distribution*, Journal of Statistics Applications and Probability, vol. 9, no. 2, pp. 319–331, 2020. doi:10.18576/jsap/090212
8. A. S. Yadav, S. S. Maiti, and M. Saha, *The inverse Xgamma distribution: statistical properties and different methods of estimation*, Annals of Data Science, vol. 8, no. 2, pp. 275–293, 2021. doi:10.1007/s40745-019-00211-w
9. S. Lee, Y. Noh, and Y. Chung, *Inverted exponentiated Weibull distribution with applications to lifetime data*, Communications for Statistical Applications and Methods, vol. 24, no. 3, pp. 227–240, 2017. doi:10.5351/CSAM.2017.24.3.227
10. A. S. Hassan, and M. Abd-Alla, *On the inverse power Lomax distribution*, Annals of Data Science, vol. 6, no. 2, pp. 259–278, 2019. doi:10.1007/s40745-018-0183-y
11. E. Chiodo, P. De Falco, L. P. Di Noia, and F. Mottola, *Inverse log-logistic distribution for extreme wind speed modeling: genesis, identification and Bayes estimation*, AIMS Energy, vol. 6, no. 6, pp. 1030–1052, 2018. doi:10.3934/energy.2018.6.1030
12. L. P. Sapkota, and V. Kumar, *Applications and some characteristics of inverse power Cauchy distribution*, Reliability: Theory & Applications, vol. 18, no. 1, pp. 301–315, 2023. doi:10.24412/1932-2321-2023-172-301-315
13. I. Elbatal, A. S. Hassan, A. M. Gemeay, L. S. Diab, A. B. Ghorbal, and M. Elgarhy, *Statistical analysis of the inverse power Zeghdoudi model: Estimation, simulation and modeling to engineering and environmental data*, Physica Scripta, vol. 99, Article 065231, 2024. doi:10.1088/1402-4896/ad46d0
14. M. Y. Awajan, D. A. Ramadan, and B. S. El-Desouky, *Inverse power modified Chris-Jerry distribution: Properties, estimation, simulation and medical application*, Applied Mathematics & Information Sciences, vol. 18, no. 6, pp. 1261–1271, 2024. doi:10.18576/amis/180608
15. A. Beghriche, Y. A. Tashkandy, M. E. Bakr, H. Zeghdoudi, A. M. Gemeay, M. D. Moyazzem Hossain, and A. H. Muse, *The inverse XLindley distribution: properties and application*, IEEE Access, 2023. doi:10.1109/ACCESS.2023.3271604
16. H. Q. Lv, L. H. Gao, and C. L. Chen, *Ailamujia distribution and its application in supportability data analysis*, Journal of Academy of Armored Force Engineering, vol. 16, no. 3, pp. 48–52, 2002.
17. A. M. El Gazar, D. A. Ramadan, M. ElGarhy, and B. S. El-Desouky, *Estimation of parameters for inverse power Ailamujia and truncated inverse power Ailamujia distributions based on progressive type-II censoring scheme*, Innovation in Statistics and Probability, vol. 1, no. 1, pp. 76–87, 2025. doi:10.18576/isp/010108
18. B. Long, *Bayesian estimation of parameter on Erlang distribution under different prior distribution*, Mathematical Practice and Theory, vol. 45, no. 4, pp. 186–192, 2015. doi:10.3969/j.issn.1000-0984.2015.04.025
19. L. P. Li, *Minimax estimation of the parameter of Erlang distribution under different loss functions*, Science Journal of Applied Mathematics and Statistics, vol. 4, no. 5, pp. 229–235, 2016. doi:10.11648/j.sjams.20160405.17
20. U. Jan, K. Fatima, and S. P. Ahmad, *On weighted Ailamujia distribution and its applications to lifetime data*, Journal of Statistics Applications and Probability, vol. 6, no. 3, pp. 619–633, 2017. doi:10.18576/jsap/060315
21. A. A. Rather, C. Subramanian, S. Shafi, K. A. Malik, P. J. Ahmad, B. A. Para, and T. R. Jan, *A new size biased distribution with applications in engineering and medical science*, International Journal of Scientific Research in Mathematical and Statistical Sciences, vol. 5, no. 4, pp. 75–85, 2018. doi:10.26438/ijsrmss/v5i4.7585
22. B. Jayakumar, and R. Elangovan, *A new generalization of Ailamujia distribution with applications in bladder cancer data*, International Journal of Scientific Research in Mathematical and Statistical Sciences, vol. 6, no. 1, pp. 1–8, 2019. doi:10.26438/ijsrmss/v6i1.18
23. A. Aijaz, A. Ahmad, and R. Tripathi, *Inverse analogue of Ailamujia distribution with statistical properties and applications*, Asian Research Journal of Mathematics, vol. 16, no. 9, pp. 36–46, 2020. doi:10.9734/arjom/2020/v16i930218
24. A. M. El Gazar, M. ElGarhy, and B. S. El-Desouky, *Classical and Bayesian estimation for the truncated inverse power Ailamujia distribution with applications*, AIP Advances, vol. 13, no. 12, Article 125122, 2023. doi:10.1063/5.0174794
25. S. T. Dara, and M. Ahmad, *Recent Advances in Moment Distribution and Their Hazard Rates*, Lap Lambert Academic Publishing GmbH KG, 2012.
26. D. V. Lindley, *Fiducial distributions and Bayes' theorem*, Journal of the Royal Statistical Society: Series B (Methodological), vol. 20, no. 1, pp. 102–107, 1958. doi:10.1111/j.2517-6161.1958.tb00278.x
27. M. M. Abdelwahab, D. A. Ramadan, S. Kumar, M. M. Hasaballah, and A. M. El Gazar, *Statistical analysis of the induced Ailamujia lifetime distribution with engineering and biomedical applications*, Mathematics, vol. 13, no. 20, Article 3307, 2025. doi:10.3390/math13203307
28. J. A. Greenwood, J. M. Landwehr, N. C. Matalas, and J. R. Wallis, *Probability weighted moments: Definition and relation to parameters of several distributions expressible in inverse form*, Water Resources Research, vol. 15, no. 5, pp. 1049–1054, 1979. doi:10.1029/WR015i005p01049
29. A. Rényi, *On measures of entropy and information*, in Proceedings of the Fourth Berkeley Symposium on Mathematical Statistics and Probability, Volume 1: Contributions to the Theory of Statistics, University of California Press, vol. 4, pp. 547–562, 1961.
30. C. Tsallis, *Possible generalization of Boltzmann–Gibbs statistics*, Journal of Statistical Physics, vol. 52, no. 1–2, pp. 479–487, 1988. doi:10.1007/BF01016429
31. J. J. Swain, S. Venkatraman, and J. R. Wilson, *Least squares estimation of distribution functions in Johnson's translation system*, Journal of Statistical Computation and Simulation, vol. 29, no. 4, pp. 271–297, 1988. doi:10.1080/00949658808811063
32. S. J. Press, *Subjective and Objective Bayesian Statistics: Principles, Models, and Applications*, John Wiley & Sons, 2009.

33. R. C. H. Cheng, and N. A. K. Amin, *Estimating parameters in continuous univariate distributions with a shifted origin*, Journal of the Royal Statistical Society: Series B (Methodological), vol. 45, no. 3, pp. 394–403, 1983. https://www.jstor.org/stable/2345281
34. B. Ranneby, *The maximum spacing method: An estimation method related to the maximum likelihood method*, Scandinavian Journal of Statistics, vol. 11, no. 2, pp. 93–112, 1984. doi:10.2307/4615946
35. E. J. G. Pitman, *Some Basic Theory for Statistical Inference*, Chapman and Hall, 1979.
36. R. C. H. Cheng, and L. Traylor, *Non-regular maximum likelihood problems*, Journal of the Royal Statistical Society: Series B (Methodological), vol. 57, no. 1, pp. 3–24, 1995. doi:10.1111/j.2517-6161.1995.tb02012.x
37. T. N. Sindhu, E. M. Almetwally, A. Shafiq, and T. A. Abushal, *Theory, simulation, and application of the entropy transformation of the Chen distribution to enhance interdisciplinary data analysis*, Journal of Radiation Research and Applied Sciences, vol. 18, no. 2, Article 101472, 2025. doi:10.1016/j.jrras.2025.101472
38. A. J. Lemonte, W. Barreto-Souza, and G. M. Cordeiro, *The exponentiated Kumaraswamy distribution and its log-transform*, Brazilian Journal of Probability and Statistics, vol. 27, no. 1, pp. 31–53, 2013. doi:10.1214/11-BJPS149
39. M. M. Nassar, and M. Ibrahem, *A new generalization of the Moyal distribution*, Journal of Statistics Applications and Probability, vol. 9, no. 2, pp. 361–378, 2020. doi:10.18576/jsap/090214
40. M. Elgarhy, R. H. Khashab, M. Ahsan-ul-Haq, M. Ibrahim, G. A. Marei, and N. M. Elharoun, *A new flexible unit Haq distribution with entomology and biomedical applications*, Statistics, Optimization & Information Computing, vol. 16, no. 6, pp. 5776–5798, 2026. doi:10.19139/soic-2310-5070-4777
41. M. Elgarhy, N. F. Hekal, M. M. El Genidy, A. R. Mohamed, and K. M. A. Mahfouz, *A new generalization of double XRamma distribution: Statistical properties and applications to real data*, Statistics, Optimization & Information Computing, vol. 16, no. 5, pp. 5220–5246, 2026. doi:10.19139/soic-2310-5070-4522
42. A. R. El-Alosey, M. Elgarhy, and A. M. Gemeay, *A new unit generated family of distributions: Classical estimation methods and applications to real data*, Statistics, Optimization & Information Computing, vol. 16, no. 5, pp. 4202–4243, 2026. doi:10.19139/soic-2310-5070-4464
43. F. C. Opone, K. Karakaya, and F. E. Osagiede, *The inverse Burr log-logistic distribution: Properties, applications and different methods of estimation*, Reliability: Theory & Applications, vol. 18, no. 1 (72), pp. 500–515, 2023.
44. C. Taniş and K. Karakaya, *A comparison of estimation methods for one parameter inverse Gompertz distribution*, Journal of Science and Arts, vol. 21, no. 3, pp. 659–668, 2021.